The effect of coupling of tectonic compression and overpressure on porosity of deep reservoirs: a case study of southern margin of Junggar Basin, northwest China

Fengqi Zhang[1,2]*, Murray Gingras[3], Chundi Shan[3], Xuesong Lu[4], Qingong Zhuo[4] and Hongli Zhong[5]

[1]School of Earth Sciences and Engineering, Xi'an Shiyou University, Xi'an, China, [2]Shaanxi Key Laboratory of Petroleum Accumulation Geology, Xi'an Shiyou University, Xi'an, China, [3]Earth and Atmospheric Sciences, Faculty of Science, University of Alberta, Edmonton, AB, Canada, [4]Research Institute of Petroleum Exploration and Development, Beijing, China, [5]Gollege of Geology and Environment, Xi'an University of Science and Technology, Xi'an, China

The majority of high quality clastic reservoirs in the foreland basins, northwest China have anomalously high primary porosity. The intensive tectonic compression, overburden and overpressure importantly impact on the deep reservoir quality in the foreland basins, and that very little research had been so far conducted on this topic. Only considering mechanical compaction without chemical diagenesis, various geological models of tectonic compression, overpressure and porosity were simulated using a comprehensive numerical model. Based on the simulations, the influences of the coupling tectonic compression and overpressure on porosity in deep reservoirs are quantitatively discussed. A case study using a representative well in the thrust belt of the Junggar foreland basin is simulated. The results show that the porosity formed from the early-middle slow burial and late rapid burial type is higher than the almost constant burial type and the early rapid burial and then slow burial type, when the overpressure is formed by the three burial types couple with the same tectonic compression. Importantly, overpressure formed during the early-middle slow burial and late rapid burial type in concert with tectonic compression best preserves high porosity within reservoirs. Either increasing tectonic compression stress early at constant overpressure or increasing the tectonic compression stress at a relative late stage and increasing reservoir overpressure can contribute to porosity loss. The porosity decreases more rapidly in the former case. The later the tectonic compression was applied, the more rapidly porosity of the reservoir decreased. Therefore, late stage tectonic compression accompanied by overpressure has the largest influence on the porosity. The porosity of the Qigu Formation in the well Ds1 in the south margin of Junggar Basin, for example, was decreased by 0.88% in response to intensive tectonic compression in the late Himalayan orogeny. However, porosity formed by overpressure suppression and preservation in the reservoir is 3.66%. So, in addition to vertical compaction and diagenesis, the influence of tectonic compression and overpressure should also be considered in the study of deep reservoir porosity evolution in foreland basin. This study can be helpful for deeply understanding the evolution rule of deep reservoir porosity in foreland basin.

KEYWORDS

tectonic compression, overpressure, porosity, foreland basin, Junggar Basin

1 Introduction

Foreland basin is one of the most abundant petroliferous basins in the world (Zhang et al., 2015; Zou et al., 2015). In recent years, large oil and gas in the deep clastic reservoirs of the foreland basins, western China are proved (Du et al., 2019; Yu et al., 2019; He et al., 2021), and these reservoirs have suffered intensive tectonic compressive processes in the late Himalayan period (Song et al., 2012; Jia et al., 2013). Because the intensive tectonic compression has an important influence on the development and preservation of porosity in reservoirs (Shou et al., 2006; Sun et al., 2013; Guo et al., 2016b; Gao et al., 2017; Mao et al., 2017; Obradors-Prats et al., 2017), in general, porosity of the reservoirs reduce as the magnitude of tectonic compression increase (Shou et al., 2006; Yang et al., 2016), and these reservoirs should be very lower porosity due to the strong compaction from the intensive tectonic compression and deep burial (Zhang et al., 2012a; Yuan et al., 2015; Feng et al., 2016). However, exploration and research in recent years show that the majority of high quality clastic reservoirs in these foreland basins have anomalously high primary porosity (Liu et al., 2019; Tian et al., 2020; Gao et al., 2023). It is difficulty to explain this phenomenon.

According to previous studies, the influence degree of tectonic compression on porosity in reservoirs nearly relates to some factors such as the size of tectonic stress, the style of tectonic deformation, the duration of tectonic compression and tectonic style and so on (Christine et al., 2010; Laubach et al., 2010; Yang et al., 2016; Obradors-Prats et al., 2017). In general, the greater the tectonic compressive stress, the faster porosity decreases (Han et al., 2015; Yang et al., 2016; Obradors-Prats et al., 2017). In addition, reservoirs in foreland basins often develop overpressure (Zhang et al., 2012a; 2012b; Luo, 2013; Wang et al., 2015). The evolution of overpressure plays a key role for the development and preservation of porosity (Bloch et al., 2002; Nguyen et al., 2013; Grant et al., 2014; Han et al., 2015; Guo et al., 2016; Lv et al., 2022). Overpressure that develops at different burial/tectonic phases has different impacts on the quality of reservoir, and most researchers suggest that high porosity is preserved in reservoirs if the overpressure formed early (Nguyen et al., 2013; Stricker et al., 2016). As suggested above, tectonic compression is also the basis for overpressure in foreland-basin reservoirs except for stress related to overburden (Zhang et al., 2011; Guo et al., 2016b; Obradors-Prats et al., 2017; Nikolinakou et al., 2018; Berthelon et al., 2021; Zhang et al., 2021; Michael and Floarin, 2022; Wang et al., 2022). The change of the porosity is controlled by the mean effective stress under the influence of the lateral and vertical compaction. The effective stress is mainly controlled by the combination of the tectonic stress, overburden and overpressure (Luo, 2004; Obradors-Prats et al., 2017). To study of the effect of tectonic compression and overpressure on porosity, previous researches mainly use the methods such as geological analyses (Shou et al., 2006; Guo et al., 2016a; 2016b; Yang et al., 2016; Mao et al., 2017; Obradors-Prats et al., 2017), physical simulations (Gao et al., 2017), and numerical models (Obradors-Prats et al., 2016; 2017; Luo et al., 2017; Nikolinakou et al., 2018) and so on. Geological analyses are mostly qualitative, and some conditions of physical simulation, such as applying of tectonic stress and assessing the internal pressure of rocks are difficult to achieve. In many respects numerical simulations provide a superior method, because this method can achieve the quantitative evolution

analysis of the porosity. Luo (2004) combined tectonic stress and hydrodynamic equations and thereby proposed the numerical simulation analysis for the effect of tectonic compression on pore pressure. Obradors-Prats et al. (2016, 2017), Nikolinakou et al. (2018) and Luo et al. (2017) used geomechanical modeling of pore pressure to quantify the effect of tectonic compression on porosity. This paper simulates various geological models that consider the co-evolution of tectonic compression and overpressure on porosity in reservoirs. Based on these simulations, the influence of the tectonic compression and overpressure on porosity in reservoirs is quantitatively discussed. To consider the numerical model, a case study using a representative well in the thrust belt of the Junggar Basin is simulated. The results of this study can contribute to a better understanding to the influence of the tectonic compression and overpressure on the development of high quality reservoirs in foreland basins, and also provide a technical means of predicting the distribution of better quality reservoirs in the deep basin.

2 Method of numerical simulation

The compaction of sediments and porosity loss are principally vertical in extensional settings. Overpressure will be generated by disequilibrium compaction when sediments undergoing burial cannot de-water fast enough for the pore fluid to remain at hydrostatic as the vertical stresses increasing (Gutierrez and Wangen., 2005; Tingay et al., 2009; Couzens-Schultz and Azbel, 2014). In compressional settings, the maximum principal stress is horizontal and the compaction of sediments and porosity change are controlled by the mean effective stress, which is closely related to the overburden, overpressure and the lateral compressional stresses, acting on the sediments (Luo, 2004; Couzens-Schultz and Azbel, 2014; Obradors-Prats et al., 2017). The numerical simulation used here combines the quantitative model of the tectonic stress with the quantitative model of the effect of tectonic stress on the porosity and the fluid dynamics equation (Luo, 2004). The solution of some parameters, such as formation pressure and formation porosity, are solved by using iteration method. This provides a quantitative simulation method for the analysis on the effect of tectonic compression and overpressure on porosity of layers.

2.1 Model of tectonic stress

Based on the assumption of the horizontal principal stress generated by gravity paralleling to the tectonic stress, three perpendicular principal stresses can be expressed as (Luo, 2004):

$$\sigma_v = \rho g h \qquad (1)$$
$$\sigma_H = v \bullet \sigma_v + \sigma_T \qquad (2)$$
$$\sigma_h = v \bullet \sigma_v \qquad (3)$$

where σ_v is the vertical load stress, ρ is the average density of rock, g is the gravitational acceleration, h is the depth, v is the coefficient of stress ratio, σ_H is the horizontal maximum principal stress, σ_h is the

horizontal minimum principal stress and σ_T is the tectonic compression stress. In this case, the following equation can be described the mean effective stress ($\bar{\sigma}'$):

$$\bar{\sigma}' = \frac{1}{3} \left(\sigma_v + 2\nu\sigma_v + \sigma_T \right) - P \tag{4}$$

where P is the pore pressure. The tectonic compression stress (σ_T) in this equation is a function of depth when the depth is shallow, but if the depth is deeper than a certain value, normally at great burial depths, it will be a constant (Luo, 2004). Those can be expressed formally by the equation:

$$\begin{cases} \sigma_T = \sigma_{Tmax} \bullet e^{b(z - z_m)}, & z < z_m, \\ \sigma_T = \sigma_{Tmax}, & z \geq z_m, \end{cases} \tag{5}$$

where σ_{Tmax} is the maximum tectonic compression stress, z_m is the given depth and b is an empirical coefficient.

2.2 Model of porosity influenced by tectonic stress

Based on previous studies, the porosity in sediments is affected not only by overburden, but also by tectonic stress and overpressure (Luo, 2004; Couzens-Schultz and Azbel, 2014; Obradors-Prats et al., 2017). Hence, when the porosity in sediments is calculated, the mean effective stress under the function of overburden, horizontal tectonic stress and overburden should be considered (Luo, 2004). The porosity in sediments can be determined as follows (Luo, 2004):

$$\Phi = \Phi_0 e^{\left[\frac{-c}{\rho_b (1 + 2\nu)/3 - \rho_f} \right] \frac{\bar{\sigma}'}{g}} \tag{6}$$

where the Φ is the porosity at a given depth, Φ_0 is the uncompacted porosity, c is a coefficient of compaction, which obtains from the relationship between porosity and depth, ρ_b is the density of sediments and ρ_f is the density of pore fluid.

2.3 Model of pore pressure influenced by tectonic stress

Using the mean stress to replace the vertical stress, the hydrodynamic equation becomes:

$$\left(\beta \bullet \Phi + \beta_s \right) \frac{dP}{dt} = \frac{1}{\rho_f} \bullet \nabla \bullet \left[\frac{k \bullet \rho_f}{\mu} \left(\nabla P - \rho_f \bullet \vec{g} \right) \right] + \beta_s \bullet \frac{d\bar{\sigma}}{dt} + \alpha \bullet \Phi \bullet \frac{dT}{dt} + Q \tag{7}$$

where the β is the compressibility of fluid, β_s is the compressibility of rock, k is the permeability, μ is the dynamic viscosity of fluid, t is the time, $\bar{\sigma} = \bar{\sigma}' + P$ is the mean stress, α is the coefficient of thermal expansion of fluid, T is the temperature and Q is the volume increase rate per unit volume (Wang et al., 1997; Luo, 2004). The permeability (k) in this equation can be solved by a simplified Kozeny-Carman equation (Luo, 2004):

$$k = \lambda' \bullet \Phi^n \tag{8}$$

where λ' is the coefficient of permeability, n is an empirical coefficient which is approximate 5.0 (Luo, 2004), and $n=5.0$. The

temperature (T) in the Equation 7 can be calculated from the heat conductivity law:

$$q = -\lambda \bullet \nabla T \tag{9}$$

where q is the heat flow, λ is the thermal conductivity tensor, ∇T is the temperature gradient. The thermal conductivity tensor can be calculated by the equation (Hantschel and Kauerauf, 2009):

$$\lambda = \lambda_r^{(1 - \Phi)} \bullet \lambda_w^{\Phi} \tag{10}$$

where λ_r is the thermal conductivity of rock, λ_w is the thermal conductivity of water. Both of the λ_r and the λ_w are the function with the temperature (Hantschel and Kauerauf, 2009), and the λ_r and the λ_w can be calculated using the equation:

$$\lambda_r = A \bullet T^2 + B \bullet T + C \tag{11}$$

where A, B and C is the constant for a rock.

$$\lambda_w = -7.23 \times 10^{-6} \bullet T^2 + 1.88 \times 10^{-3} \bullet T + 0.565 \,\text{for}\, T < 137^{\circ}C$$
$$\lambda_w = -5.14 \times 10^{-6} \bullet T^2 + 1.31 \times 10^{-3} \bullet T + 0.602 \,\text{for}\, T > 137^{\circ}C \tag{12}$$

Assuming the λ_r and the λ_w is constant for a given layer in the vertical direction (Hantschel and Kauerauf, 2009), they can be calculated from the upper layer on the condition of known surface temperature. Then the temperatures of every stratum can be ultimately calculated from top to bottom.

The complicated Eq. 7 above can be solved using cyclic iteration. The pore pressure and porosity in sediments under the different tectonic compression conditions in the geological history are recovered using the numerical simulation. This modeling only considers mechanical compaction without chemical diagenesis.

3 Numerical simulation considering the coupling of tectonic compression and overpressure on porosity

By classifying the representative sedimentation and tectonic evolution of foreland basins, some classic patterns of the coupling of tectonic stress and overpressure can be summarized. These different patterns relate to various evolutions of the porosity of reservoirs due to different processes. Firstly, the evolution of overpressure, which is formed by different burial types, can couple with the contemporaneous tectonic stress of a similar magnitude. Secondly, the overpressure formed by the same burial types coupled with the different magnitudes of contemporaneous tectonic stress. Thirdly, tectonic stress formed in different periods coupled with the overpressure formed by the same burial processes in the same layer assemblages.

3.1 Coupling of tectonic stress and overpressure formed by different burial types and its effect on porosity in reservoirs

Based on previous efforts (He et al., 2010; Feng et al., 2016), the burial process of sediments in sedimentary basins can be grouped into three common types: early-middle slow burial and late rapid burial (Type 1), almost constant burial (Type 2) and early rapid
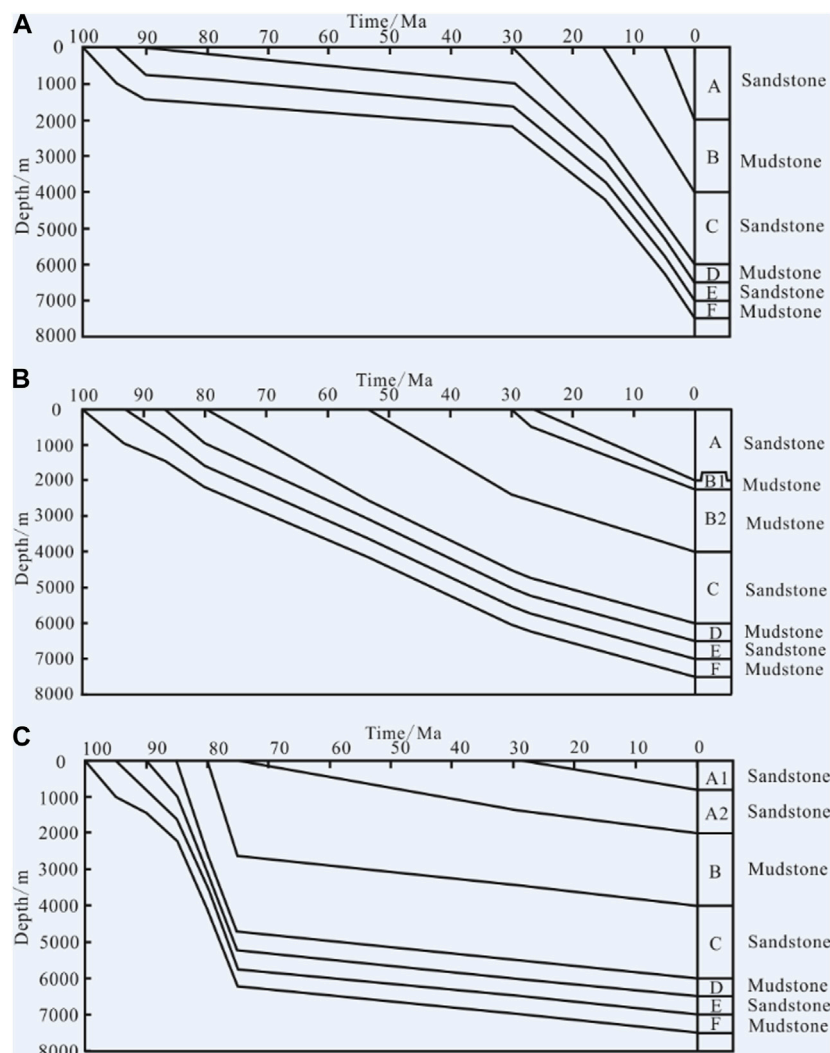
FIGURE 1
(A) Burial history of the Model 1. **(B)** Burial history of the Model 2. **(C)** Burial history of the Model 3.

burial and then slow burial (Type 3). These burial types are illustrated in Figures 1A, B, C, respectively. Using these three different burial types, various geological models can be considered and the different developmental paths of overpressure can be modeled (*i.e.*, Model 1, Model 2 and Model 3).
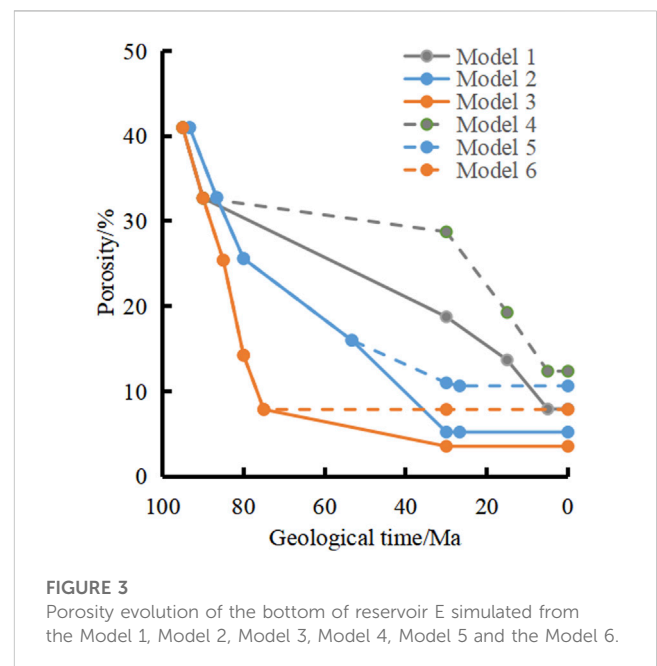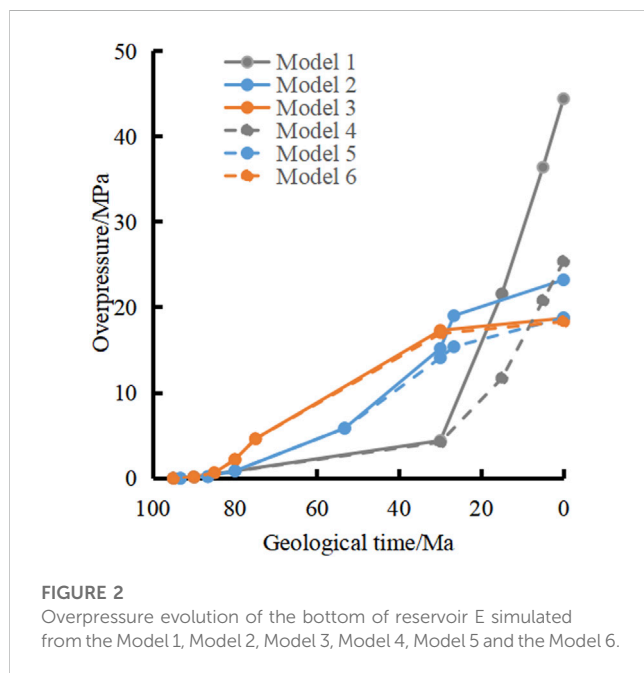
The three models (Models 1, 2 and 3) and their lithologies are shown in Figure 1 and summarized in Table 1. The tectonic stress conditions applied to the three models are the maximum tectonic stress (σ_{Tmax}), which is 200 MPa from 30 Ma to the present-day. Also, models 1, 2 and 3 correspond respectively to models 4, 5 and 6, which do not consider the tectonic stress but only consider the overburden stress: this permits comparison of overpressure and porosity under the two conditions for each burial type. For each of these simulations, the uncompacted porosity of sandstone and mudstone are 41% and 70% respectively, their coefficients of compaction are 0.00031 m^{-1} and 0.00083 m^{-1} respectively. Coefficient of stress ratio (ν) in each model is 0.82 (Luo, 2004), coefficients of permeability (λ') for sandstone and mudstone are 10^{-11} m^2 and 10^{-16} m^2 respectively, compressibilities of sandstone

and mudstone (β_s) are 3.9×10^{-11} m^2 and 5.5×10^{-11} Pa^{-1} respectively and the compressibility of fluid (β) in each model is 4.8×10^{-10} Pa^{-1}. The z$_m$ in each model is 10000m, and the coefficient of thermal expansion of fluid (α) is 5.0×10^{-4}°C^{-1}. The A, B, C in the Eq. 11 for sandstone and mudstone in each model are 0.00001, −0.0081, 4.0991 and −0.000001, 0.0008, 1.626 respectively. The heat flow (q) and surface temperature in all periods of each model is 42 mW/ m^2 and 16°C respectively. Setting the bottom of reservoir E as an observation point, the results of simulation are assessed.

The results of the simulations indicate that there are different evolutionary paths between followed by overpressure and porosity in reservoirs characterized by different burial types. Following burial Type 3, the overpressure in reservoir E is 4.5 MPa higher than burial Type 2 (Model 2 and Model 3; Figure 2). Overpressure in reservoir E formed by burial Type 1 is higher yet by about 21 MPa (Model 1 and Model 2; Figure 2). The porosity of reservoir E in the three different burial models shows clear differences. The magnitude order is burial Type 1 > burial Type 2 > burial Type 3, and differences between them are 2.7% and 1.7% successively (Figure 3). Those porosity

TABLE 1 The main parameters of Models 1, 2, 3, 4, 5, 6, 7, 8, 9, 10, 11, 12 showing the burial process, the magnitudes and the periods of tectonic stress, the uncompacted porosity and the coefficients of compaction and the coefficients of permeability for sandstone and mudstone.

Geological model	Burial process	Maximum tectonic stress applied on the models (MPa)	Periods of tectonic stress (Ma)	Uncompacted porosity of sandstone and mudstone (%)	Coefficients of compaction for sandstone and mudstone (m^{-1})	Coefficients of permeability for sandstone and mudstone (m^2)
Model 1	Type 1	200	30~0	41, 70	0.00031, 0.00083	10^{-11}, 10^{-16}
Model 2	Type 2					
Model 3	Type 3					
Model 4	Type 1	0	30~0			
Model 5	Type 2					
Model 6	Type 3					
Model 7	Type 2	0	26.7~0			
Model 8		150				
Model 9		300				
Model 10	Type 1	200	31~16			
Model 11			16~6			
Model 12			6~0			

FIGURE 2
Overpressure evolution of the bottom of reservoir E simulated from the Model 1, Model 2, Model 3, Model 4, Model 5 and the Model 6.

FIGURE 3
Porosity evolution of the bottom of reservoir E simulated from the Model 1, Model 2, Model 3, Model 4, Model 5 and the Model 6.

differences between each burial type are mainly caused by the forming of overpressure, which suppressed on the compaction of reservoir. Comparing overpressure and porosity of a reservoir under constant tectonic stress (models 1, 2 and 3) with values neglecting tectonic stress (models 4, 5 and 6), both of overpressure and porosity are changed by tectonic compression. Porosity of reservoirs decrease whereas overpressure of reservoirs increase. The overpressure at the bottom of reservoir E between these two conditions (tectonic stress *versus* no tectonic stress) is Type 1 > Type 2 > Type 3, and the changing values between the two are 19.0 MPa, 4.4 MPa and

0.4 MPa respectively (Figure 2). The porosity at the bottom of reservoir E comparing the same two conditions is Type 2 > Type 1 > Type 3, and the changing values between them are 5.4%, 4.4% and 4.3% respectively (Figure 3).

Therefore, the coupling of a late-stage constant tectonic stress with overpressure formed by different burial types will lead to different magnitudes of porosity reduction in deep-basin reservoirs. Among these burial types, Type 1 will retain the largest porosity and has the best prospect to preserve high porosity.
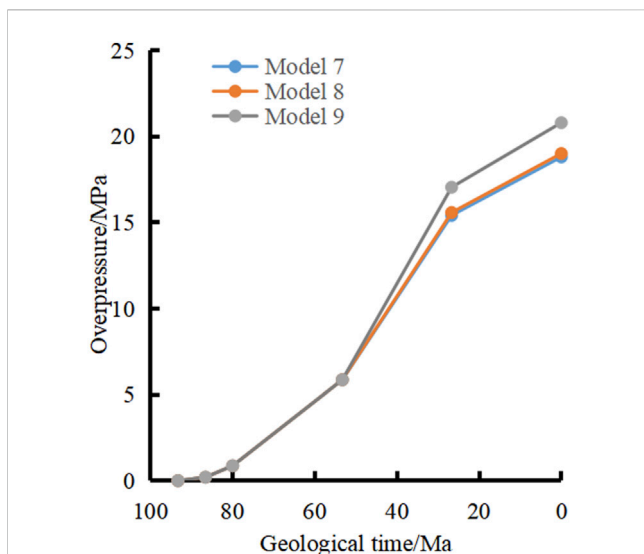
FIGURE 4
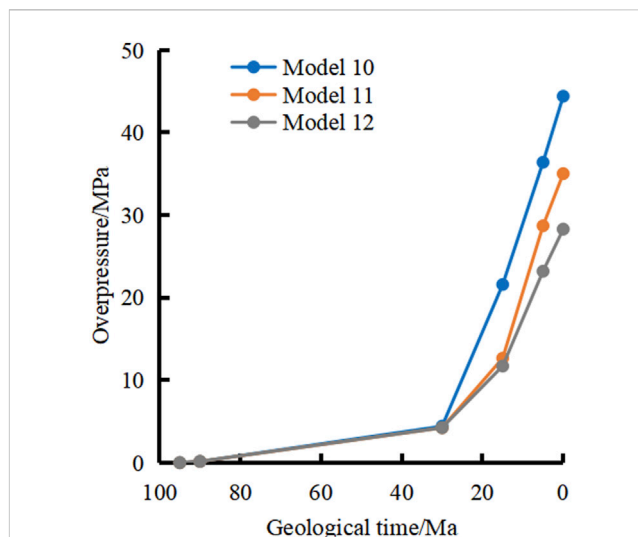Overpressure evolution of the bottom of reservoir E simulated from the Model 7, Model 8, Model 9.

FIGURE 6
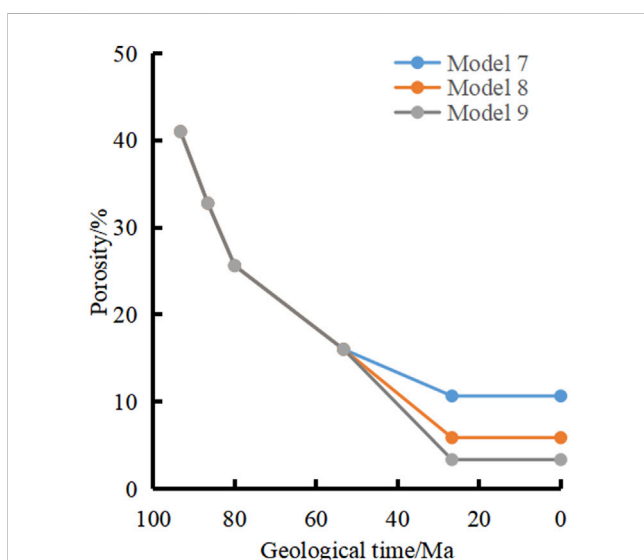Overpressure evolution of the bottom of reservoir E simulated from the Model 10, Model 11, Model 12.

FIGURE 5
Porosity evolution of the bottom of reservoir E simulated from the Model 7, Model 8, Model 9.

3.2 Coupling of different tectonic stress and overpressure and its effect on porosity of reservoirs

Using models 2 as a basis, we apply tectonic stress values (σ_{Tmax}) of 0 MPa, 150 MPa and 300 MPa respectively during 27 Ma to 0 Ma and are presented as models 7, 8 and 9 respectively. The coefficients of stress ratio (ν) and the coefficients of permeability (λ) for each lithology are held the same as in Model 2. By applying the different magnitudes of contemporaneous tectonic stress, their effect on overpressure and porosity of reservoirs can be studied.

Comparing the overpressure and the porosity in Model 7 (σ_{Tmax}=0 MPa) to Model 8 (σ_{Tmax}=150 MPa), the modeled overpressure of reservoir E in Model 8 is slightly greater (0.2 MPa) than Model 7 (Figure 4). However, Model 8 porosity is reduced to 4.8% (Figure 5). The results of the simulation show that although the tectonic stress is small, the porosity will decrease with increasing tectonic compression at the same time, the overpressure changes far less dramatically. Comparing Model 7 and Model 8 with Model 9, which is characterized by the greatest tectonic compression (σ_{Tmax}=300 MPa), both the overpressure and the porosity of reservoir E change notably. The porosity of reservoir E in Model 9 decreases by approximately 2.5% compared to Model 8 (Figure 5), but the overpressure of reservoir E increases 1.8 MPa (Figure 4). Thus, we can conclude that although the change in tectonic stress in Model 7 to Model 8 and Model 8 to Model 9 are equal, the rate of porosity change is different. The porosity decreases faster before the overpressure caused by tectonic compression begins to develop.

When the tectonic compression is increasing and exceeds a certain value (i.e., σ_{Tmax} is approximately equal to 150 MPa), both the overpressure and porosity of reservoirs will be changed: porosity will decrease whereas overpressure increases. There are two coupling ways. The first one is increasing of tectonic stress at a relative early stage and without changing of reservoir overpressure, the second one is increasing of tectonic stress at a late stage and increasing of reservoir overpressure. Overall, the porosity decreases more rapidly when early tectonic stress is applied.

3.3 Coupling of tectonic stress in different periods and overpressure and its effect on porosity of reservoirs

The conditions of burial Type 1 for this simulation are presented below. They are a constant maximum tectonic stress value (σ_{Tmax}=200 MPa) at periods of 31-16 Ma, 16-6 Ma and 6-0 Ma
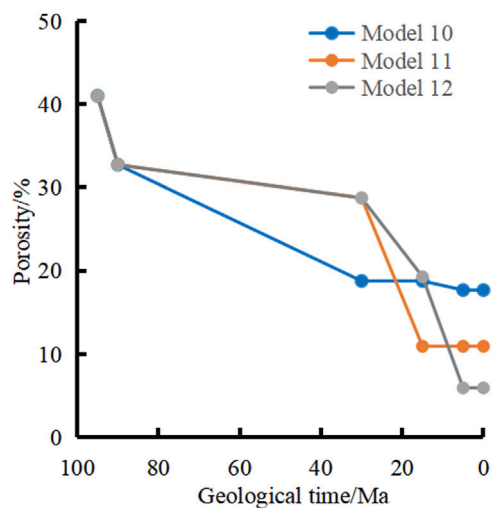
FIGURE 7
Porosity evolution of the bottom of reservoir E simulated from the Model 10, Model 11, Model 12.

respectively, and presented as models 10, 11 and 12 respectively. The coefficients of stress ratio (v), the coefficients of permeability (λ') for each lithology in these models are the same as Model 1. These model constraints are used to determine the overpressure and porosity effects of the same magnitude of tectonic stress over different periods of time. For the results of simulation, after applying 200 MPa of the maximum tectonic stress in different periods, overpressures in reservoir E at present between them have large difference. The overpressure of reservoir E at the present-day has the highest value (44.4 MPa) if the tectonic stress was applied in an earlier in the Model 10, and it has the lowest value (28.3 MPa) if a later tectonic stress was applied on the Model 12 (Figure 6). The porosity of reservoir E at the present-day between them also shows large differences. The porosity of reservoir E is highest (17.7%) if the tectonic stress is applied early. The porosity is lowest (5.9%) if a late tectonic stress is applied as with Model 12 (Figure 7).

Based on the above, the later the tectonic stress is applied, the greater the porosity of reservoirs is decreased. If the tectonic stress is applied early, overpressure will also develop early, and so high porosity is easier to preserve due to the suppression of overpressure in the reservoirs. Therefore, the coupling way of early tectonic stress and overpressure has the best potential to form and preserve high porosity within a deep reservoir. The combination of late tectonic stress and overpressure has the largest impact on the porosity and that is not favorable for the preservation of high porosity.

4 Case study

The south margin of Junggar Basin is located next to the North Tianshan Mountains. This part of the basin has gone through three tectonic evolutionary stages: a foreland-basin stage (from the Permian to the Triassic), intracontinental depression basin stage (from the Jurassic to the Paleogene) and a rejuvenated foreland-basin stage (since the Neogene) (Wang et al., 2005). The south margin of the Junggar Basin suffered intensive tectonic compression caused by the rapid uplift of North Tianshan Mountains, which is a consequence of the Indian-Eurasian collision in the Neogene (Wang et al., 2005). The largest lateral tectonic stress field was formed during this event (Wu et al., 2000). In the south margin of Junggar Basin, overpressure is commonly developed in the Mesozoic and the Cenozoic (Xu et al., 2000; Wang et al., 2003; Yang et al., 2012). The strong tectonic compression has a significant impact on the forming of overpressure (Luo et al., 2007; Zhang et al., 2011; Zhang et al., 2012a), and lead to a decrease of porosity in sediments in the study area (Shou et al., 2006; Gao et al., 2017; Mao et al., 2017; Obradors-Prats et al., 2017). As further exploration occurs in the study area, the targets of exploration are gradually shifting to deeper strata such as the so-called lower play (Shao, 2013). Overpressure also exists at these depths.

However, what is the effect of tectonic compression on overpressure and the formation and preservation of high quality reservoirs in the study area? Unfortunately, a clear answer to this question is still unavailable. In this case study, the well Ds1, which has been drilled to the lower play, can be used to assess the effect of tectonic compression on overpressure and porosity. The well Ds1 is located in the anticline of Dushanzi area near the eastern part of Sikeshu sag in the south margin of Junggar Basin and the layers drilled by this well include Jurassic Qigu (J_3q), Cretaceous Qingshuihe (K_1q), Hutubi (K_1h), Shengjinkou (K_1s), Lianmuqin (K_1l), Donggou (K_2d), Paleogene Ziniquanzi ($E_{1-2}z$), Anjihaihe ($E_{2-3}a$), Neogene Shawan (N_1s), Taxihe (N_1t), Dushanzi (N_2d) formations and undifferentiated Quaternary strata. In those formations, the Jurassic Qigu formation and lower part of Cretaceous Qingshuihe formation are the main unit for exploration. The Lower Cretaceous Tugulu group including K_1q, K_1h, K_1s, K_1l provide important cap rocks. The Jurassic Badaowan (J_1b) Formation and Xishanyao (J_2x) Formation are the major hydrocarbon source rocks of the lower play (Wei et al., 2010; Tian et al., 2017). For the purpose of understanding the magnitude of tectonic stress in the well Ds1, the lateral maximum principal stress at depth 6,417.90 m was tested by the acoustic emission (AE) (254.51 MPa) (Table 2). This value reflects the lateral maximum principal stress of that stratum from the beginning of the Neogene and especially during the Quaternary. The result show that the lateral maximum principal stress of the Qigu formation in the well Ds1 is greater than the overburden stress. During the above simulations, when a maximum tectonic stress value (σ_{Tmax}=270 MPa) during the periods from 5 Ma to 0 Ma was applied, the calculated lateral maximum principal stress is generally aligned with the measured value. Since there was also a certain tectonic compression during the Taxihe sedimentary period (Wang et al., 2005), a maximum tectonic stress value (σ_{Tmax}=100 MPa) during the periods from 16.3 Ma to 5 Ma was also applied. The condition without considering tectonic compression was also simulated to compare differences with the stressed models. Many parameters used in the simulation were assessed empirically or measured in the study area. For example, porosity and pore pressure are measured in the study area. Paleo-surface temperatures and paleo-heat flow used in the simulation are cited from the Hantschel and Kauerauf. (2009) and the Rao et al. (2013), Rao et al. (2018) respectively. They are shown in the Figure 8.

TABLE 2 The results of acoustic emission test of the well Ds1 in the study area, and the contrast and the difference of maximum horizontal principal stress and vertical principal stress.

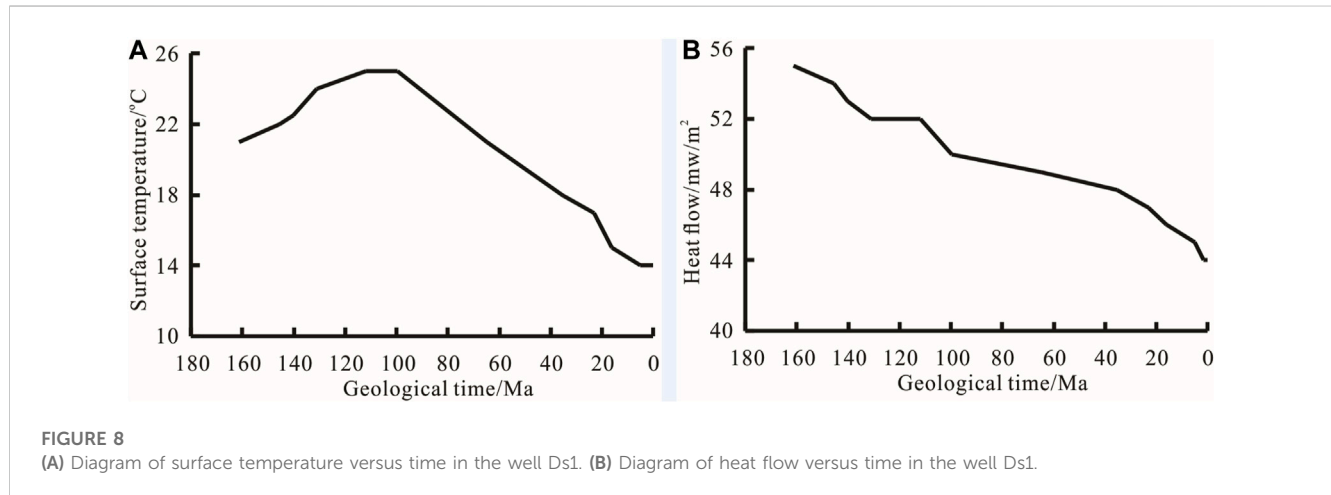| Well	Stratum symbol	Depth (m)	Maximum horizontal principal stress (σ_{hmax}) (MPa)	Vertical principal stress (σ_v) (MPa)	Contrast of σ_{hmax} and σ_v	Difference value of σ_{hmax} and σ_v (MPa)
Ds1	J_3q	6,417.90	254.51	155.60	$\sigma_{hmax} > \sigma_v$	98.90

FIGURE 8
(A) Diagram of surface temperature versus time in the well Ds1. (B) Diagram of heat flow versus time in the well Ds1.

The errors for the some parameters in the simulation were assessed. The results show that the strata in the well Ds1 experienced Type 1 burial (Figure 9A) and the simulated values of vitrinite reflectance (R_o) and formation temperature are in good agreement with the measured value (Figures 9B, C). After applying a tectonic stress, which is close to the measured data, the simulation shows that porosity of Qigu formation at present in the well Ds1 should be 5.7%. The measured porosity values in the Qigu formation of this well range from 5.8% to 7.6% and the mean value is 6.6%. According to previous studies, the reservoir pores of Qigu formation in the study area are mainly intergranular pores, accounting for about 70%–75%, and the rest are intergranular and intragranular dissolved pores and fractures (Wang et al., 2022; Gao et al., 2023). So the porosity obtained by this simulation is close to the primary intergranular porosity, and this result is reasonable. The pressure coefficient of the formation from the simulation is 1.72 and overpressure is 41.8 MPa. Because there is not any measured pressure coefficient data for this formation from the well Ds1, the data from the adjacent well Xh1, which is 2.18, is used. This simulation for overpressure is mainly generated by the disequilibrium compaction of tectonic compression and overburden. Except for these two factors, overpressure transfer also contributes to overpressure in the Qigu formation according to the former research (Luo et al., 2007; Zhang et al., 2020; 2021). So, current overpressure induced by overpressure transfer is 33.4 MPa (Figure 10). According to the previous research, the overpressure transfer mainly occurred from the end of Neogene Dushanzi to the Quaternary. The formation of anticline and the opening of fault in these periods are the main factors of overpressure transfer (Zhang et al., 2020).

As a result, the intensive tectonic compression from the Dushanzi period in the study area had a significant impact to overpressure and porosity of the Qigu formation in the lower play of the well Ds1

(Figures 10, 11). Before the formation of tectonic compression, the formation pressure in this reservoir is basically normal pressure. In the early sedimentary stage of the Shawan formation, the porosity of the Qigu formation in the well Ds1, which is 15.8%, was still high. However, in the early sedimentary stage of the Taxihe formation, the porosity of the reservoir initially decreased rapidly to 10.4% due to the moderate intensity tectonic compression, but the tectonic compression did not cause the overpressure in the reservoir. Compared with the simulation result just considering overburden stress and overpressure, the decreasing porosity caused by tectonic compression in the reservoir is 3.3% (Figure 11). After experiencing the intensive tectonic compression since the Dushanzi period, both overpressure and porosity of the Qigu formation in the well Ds1 changed substantially, and overpressure caused by tectonic compression reached the maximum value during the Quaternary. The overpressure is about 41.8 MPa and it is calculated from the comparison with the simulation that only considered overburden stress (Figure 10). Because of the coupling of intensive tectonic compression, overburden and overpressure, the porosity of the reservoir decreased rapidly and then stabilized (Figure 11). Compared with the simulation result just considering overburden stress and overpressure, the decreasing porosity caused by tectonic compression in the reservoir constantly changes, it reaches the maximum in the early stage of the Dushanzi deposition and is smaller at present-day, their sizes are 4.48% and 0.88%, respectively (Figure 11). Compared with the calculation result just considering tectonic compression stress and overburden stress, current porosity formed by overpressure suppression and preservation in the reservoir is 3.66% (Figure 11). Thus, the coupling of the intensive tectonic compression at the late Himalayan period and overpressure caused the porosity of deep
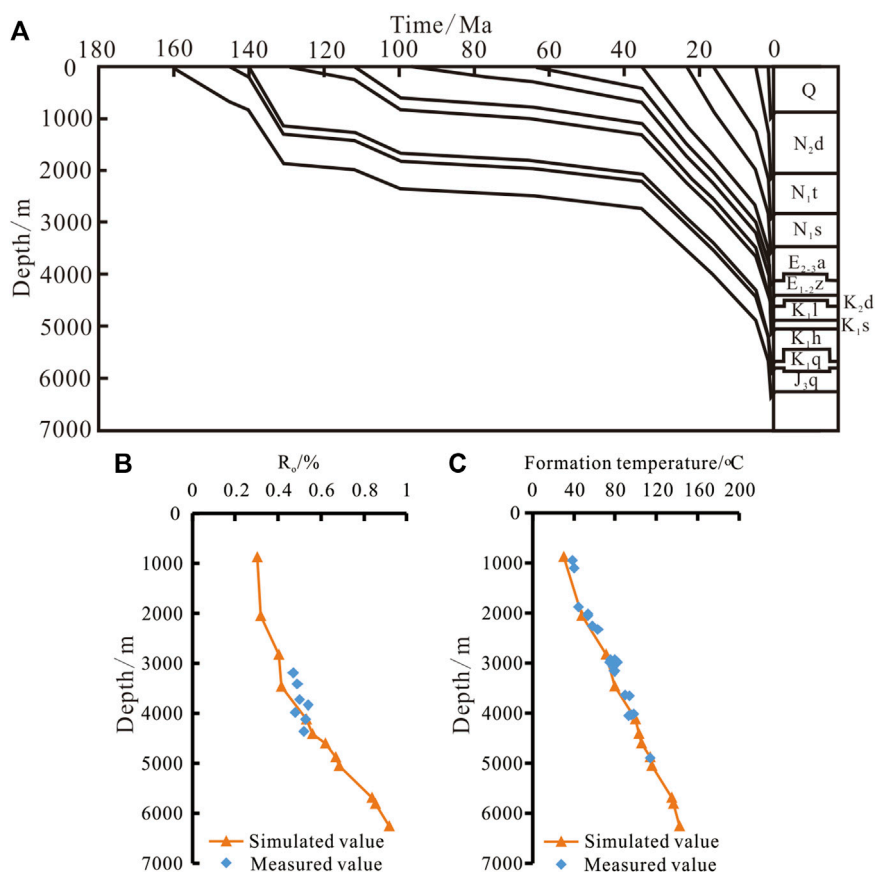
FIGURE 9
(A) Burial history of the well Ds1 in the study area. **(B)** Diagram of vitrinite reflectance versus depth of the well Ds1. **(C)** Diagram of formation temperature versus depth of the well Ds1.
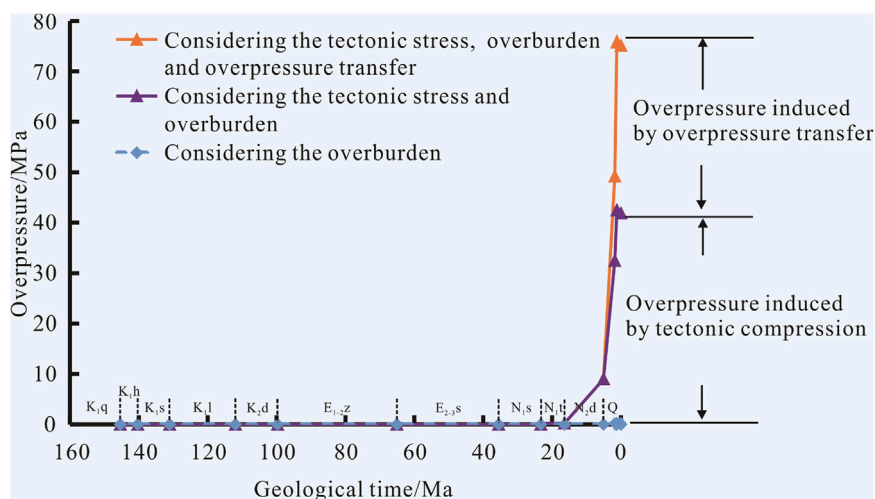

FIGURE 10
Overpressure evolution of reservoir of Qigu formation in well Ds1 of the study area, including the simulation results from considering the tectonic stress and overburden and overpressure transfer, and the tectonic stress and overburden, and the overburden.
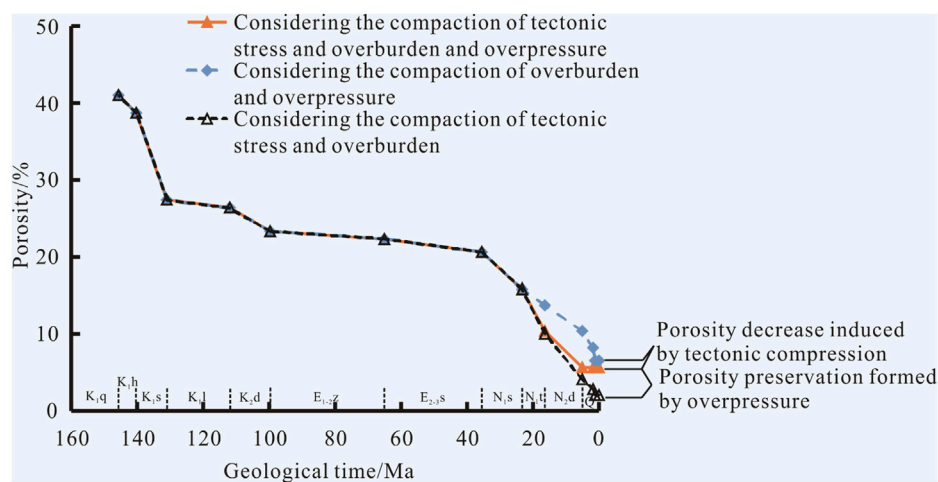
FIGURE 11
Porosity evolution of reservoir of Qigu formation in well Ds1 of the study area, including the simulation results from considering the compaction of tectonic stress and overburden and overpressure, and the compaction of overburden and overpressure, and the compaction of tectonic stress and overburden.

reservoirs in the study area decrease. However, to a certain extent, overpressure plays a good role in inhibiting and preserving the formation of abnormally high primary porosity of deep reservoir in the study area.

5 Conclusions

1) Overpressure caused by early-middle slow burial and late rapid burial type, almost constant burial type, or early rapid burial and then slow burial type are modeled with the same tectonic stress at the same model times. The early-middle slow burial and late rapid burial type preserves the greatest porosity and is the best way to preserve the abnormal high porosity of deep reservoirs.

2) Either increasing tectonic compression stress early at constant overpressure or increasing the tectonic compression stress at a relative late stage and increasing reservoir overpressure will cause a reduction of porosity. In addition, the rate of porosity change will decrease faster with early tectonic compression even when the same tectonic compression stress is applied (to the various models). So the porosity in the different stages will have different rates of change.

3) If a deep-basin reservoir is exposed to constant tectonic stress during different model times, but with the same burial type, the later the tectonic stress applied, the more the porosity is decreased. The pairing of tectonic stress in late time periods and overpressure has a larger effect on the porosity of deep reservoirs.

4) For the deep-basin reservoirs in the lower play in the south margin of Junggar Basin that experienced early-middle slow burial and late rapid burial process (Type 1), their porosity was largely decreased by the intensive tectonic compression during the late Himalayan orogeny. However, to some extent, overpressure inhibits the decrease of their porosity. This supports the assertion that intensive tectonic compression and overpressure have a significant impact on the porosity of deep reservoirs in foreland basin.

Data availability statement

The original contributions presented in the study are included in the article/Supplementary Material, further inquiries can be directed to the corresponding author.

Author contributions

FZ, MG, and CS provided the idea and writing of the manuscript; XL, QZ, and HZ provided supervision, review, data analysis and editing. All authors contributed to the article and approved the submitted version.

Conflict of interest

The authors declare that the research was conducted in the absence of any commercial or financial relationships that could be construed as a potential conflict of interest.

Publisher's note

References

Berthelon, J., Brüch, A., Colombo, D., Frey, J., Traby, R., Bouziat, A., et al. (2021). Impact of tectonic shortening on fluid overpressure in petroleum system modelling: Insights from the Neuquén basin, Argentina. *Mar. Pet. Geol.* 127, 104933–108272. doi:10.1016/J.MARPETGEO.2021.104933

Bloch, S., Lander, R. H., and Bonnell, L. M. (2002). Anomalously high porosity and permeability in deeply buried sandstone reservoirs: Origin and predictability. *AAPG Bull.* 86 (2), 301–328. doi:10.1306/61EEDABC-173E-11D7-8645000102C1865D

Christine, S., Quentin, J. F., Martin, C., and Peter, B. (2010). Structural controls on mechanical compaction within sandstones: An example from the Apsheron Peninsula, Azerbaijan. *Mar. Pet. Geol.* 27 (8), 713–724. doi:10.1016/j.marpetgeo.2010.06.010

Couzens-Schultz, B. A., and Azbel, K. (2014). Predicting pore pressure in active fold-thrust systems: An empirical model for the deepwater Sabah foldbelt. *J. Struct. Geol.* 69, 465–480. doi:10.1016/j.jsg.2014.07.013

Du, J., Zhi, D., Li, J., Yang, D., Tang, Y., Qi, X., et al. (2019). Major breakthrough of Well Gaotan 1 and exploration prospects of lower assemblage in southern margin of Junggar Basin, NW China. *Pet. Explor Dev.* 46 (2), 216–227. doi:10.1016/s1876-3804(19)60003-0

Feng, J., Gao, Z., Cui, J., and Zhou, C. (2016). The exploration status and research advances of deep and ultra-deep clastic reservoirs. *Adv. Earth Sci.* 31 (7), 718–736. doi:10.11867/j.issn.1001-8166.2016.07.0718

Gao, C., Wang, J., Jin, J., Liu, M., Ren, Y., Liu, K., et al. (2023). Heterogeneity and differential hydrocarbon accumulation model of deep reservoirs in foreland thrust belts: A case study of deep cretaceous Qingshuihe formation clastic reservoirs in southern Junggar Basin, NW China. *Pet. Explor Dev.* 50 (2), 360–372. doi:10.1016/S1876-3804(23)60393-3

Gao, Z., Cui, J., Feng, J., Zhou, C., and Shi, Y. (2017). Modification mechanism of physical properties of deeply-buried sandstone reservoir due to the burial compaction and lateral extrusion in Kuqa depression. *Geosci* 31 (2), 302–314.

Grant, N. T., Middleton, A. J., and Archer, S. (2014). Porosity trends in the Skagerrak formation, central graben, United Kingdom continental shelf: The role of compaction and pore pressure history. *AAPG Bull.* 98 (6), 1111–1143. doi:10.1306/10211313002

Guo, X., Liu, K., Jia, C., Song, Y., Zhao, M., and Lu, X. (2016a). Effects of early petroleum charge and overpressure on reservoir porosity preservation in the giant Kela-2 gas field, Kuqa depression, Tarim Basin, northwest China. *AAPG Bull.* 100 (2), 191–212. doi:10.1306/11181514223

Guo, X., Liu, K., Jia, C., Song, Y., Zhao, M., Zhuo, Q., et al. (2016b). Constraining tectonic compression processes by reservoir pressure evolution: Overpressure generation and evolution in the Kelasu Thrust Belt of Kuqa Foreland Basin, NW China. *Mar. Pet. Geol.* 72, 30–44. doi:10.1016/j.marpetgeo.2016.01.015

Gutierrez, M., and Wangen, M. (2005). Modeling of compaction and overpressure in sedimentary basins. *Mar. Pet. Geol.* 22 (3), 351–363. doi:10.1016/j.marpetgeo.2005.01.003

Han, D., Zhao, R., Li, Z., and Li, W. (2015). The characteristic of diagenetic compaction induced by multiform geodynamic mechanisms in reservoir: An example from Cretaceous sandstone reservoir in Kuqa depression, Tarim Basin. *Chin. J. Geol.* 50 (1), 241–248. doi:10.3969/j.issn.0563-5020.2015.01.015

Hantschel, T., and Kauerauf, A. I. (2009). *Fundamentals of basin and petroleum systems modeling.* Berlin: Springer.

He, H., Fan, T., Guo, X., Yang, T., Zheng, M., Huang, F., et al. (2021). Effect of *Issatchenkia terricola* WJL-G4 on deacidification characteristics and antioxidant activities of red raspberry wine processing. *Chin. Pet. Explor* 26 (1), 17–30. doi:10.3390/jof8010017

He, X., Liu, Z., Liang, Q., Li, J., and Qi, Y. (2010). The influence of burial history on mudstone compaction. *Earth Sci. Front.* 17 (4), 167–173.

Jia, C., Li, B., Lei, Y., and Chen, Z. (2013). The structure of Circum-Tibetan Plateau Basin-Range System and the large gas provinces. *Sci. China Earth Sci.* 56 (11), 1853–1863. doi:10.1007/s11430-013-4649-7

Laubach, S. E., Eichhubl, P., Hilgers, C., and Lander, R. U. (2010). Structural diagenesis. *J. Struct. Geol.* 32 (12), 1866–1872. doi:10.1016/j.jsg.2010.10.001

Liu, C., Xu, Z., Chen, G., Deng, Y., Wang, J., and Zhao, J. (2019). Hydrocarbon accumulation conditions and evolution process of the ZQ1 large condensate gas reservoir in the Qiulitage structural belt, Tarim Basin. *Nat. Gas. Ind.* 39 (4), 8–17. doi:10.3787/j.issn.1000-0976.2019.04.002

Luo, G., Hudec, M. R., Flemings, P. B., and Nikolinakou, M. A. (2017). Deformation, stress, and pore pressure in an evolving suprasalt basin. *J. Geophys Res. Solid Earth* 122 (7), 5663–5690. doi:10.1002/2016JB013779

Luo, X. (2013). Overpressuring in foreland basins: Geological affects and their efficiency. *Chin. J. Geol.* 48 (1), 32–49. doi:10.3969/j.issn.0563-5020.2013.01.002

Luo, X. (2004). Quantitative analysis on overpressuring mechanism resulted from tectonic stress. *Chin. J. Geol.* 47 (6), 1223–1232. doi:10.1002/cjg2.608

Luo, X., Wang, Z., Zhang, L., Yang, W., and Liu, L. (2007). Overpressure generation and evolution in a compressional tectonic setting, the southern margin of Junggar Basin, northwestern China. *AAPG Bull.* 91 (8), 1123–1139. doi:10.1306/02260706035

Lv, X., Fu, M., Zhang, S., Meng, X., Liu, Y., Ding, X., et al. (2022). Effect of diagenesis on the quality of high-temperature reservoirs exposed to high-temperature, overpressure, and CO_2-charging conditions: A case study of upper miocene huangliu sandstones of dongfang district, yinggehai basin, south China sea. *Front. Earth Sci.* 10, 885602. doi:10.3389/feart.2022.885602

Mao, Y., Zhong, D., Li, Y., Wang, T., Sun, H., and Wang, Y. (2017). Differential compaction of deep sandstones in compressive tectonic setting: A case study of cretaceous reservoirs in kuqa foreland thrust belt, tarim basin. *Oil Gas. Geol.* 38 (6), 1113–1122. doi:10.11743/ogg20170612

Michael, C. D., and Florian, D. (2022). Overpressure, vertical stress, compaction and horizontal loading along the North Alpine Thrust Front, SE Germany. *Mar. Pet. Geol.* 143, 105806. doi:10.1016/J.MARPETGEO.2022.105806

Nguyen, B. T. T., Jones, S. J., Gouly, N. R., Middleton, A. J., Grant, N., Ferguson, A., et al. (2013). The role of fluid pressure and diagenetic cements for porosity preservation in Triassic fluvial reservoirs of the Central Graben, North Sea. *AAPG Bull.* 97 (8), 1273–1302. doi:10.1306/01151311163

Nikolinakou, M. A., Heidari, M., Flemings, P. B., and Hudec, M. R. (2018). Geomechanical modeling of pore pressure in evolving salt systems. *Mar. Pet. Geol.* 93, 272–286. doi:10.1016/j.marpetgeo.2018.03.013

Obradors-Prats, J., Rouainia, M., Aplin, A. C., and Crook, A. J. L. (2017). Assessing the implications of tectonic compaction on pore pressure using a coupled geomechanical approach. *Mar. Pet. Geol.* 79, 31–43. doi:10.1016/j.marpetgeo.2016.10.017

Obradors-Prats, J., Rouainia, M., Aplin, A. C., and Crook, A. J. L. (2017). Hydromechanical modeling of stress, pore pressure, and porosity evolution in fold-and-thrust belt systems. *J. Geophys Res. Solid Earth* 122, 9383–9403. doi:10.1002/2017JB014074

Obradors-Prats, J., Rouainia, M., Aplin, A. C., and Crook, A. J. L. (2016). Stress and pore pressure histories in complex tectonic settings predicted with coupled geomechanical-fluid flow models. *Mar. Pet. Geol.* 76, 464–477. doi:10.1016/j.marpetgeo.2016.03.031

Rao, S., Hu, S. B., Zhu, C. Q., Tang, X. Y., Li, W. W., and Wang, J. Y. (2013). The characteristics of heat flow and lithospheric thermal structure in Junggar Basin, northwest China. *Chin. J. Geophys* 56 (8), 2760–2770. doi:10.6038/cjg20130824

Rao, S., Zhu, Y. K., Hu, D., Hu, S. B., and Wang, Q. (2018). The thermal history of Junggar Basin: Constrains on the tectonic attribute of the early-middle permian basin. *Acta Geol. Sin.* 92 (6), 1176–1195.

Shao, Y. (2013). Hydrocarbon accumulation of the Jurassic deeply-buried lower assemblage in the southern Junggar Basin. *Geol. J. China U* 19 (3), 86–94. doi:10.16108/j.issn1006-7493.2013.01.009

Shou, J., Zhang, H., Shen, Y., Wang, X., Zhu, G., and Si, C. (2006). Diagenetic mechanisms of sandstone reservoirs in China oil and gas-bearing basins. *Acta Pet. Sin.* 22 (8), 2165–2170.

Song, Y., Zhao, M., Fang, S., Xie, H., Liu, S., and Zhuo, Q. (2012). Dominant factors of hydrocarbon distribution in the foreland basins, central and Western China. *Pet. Explor Dev.* 39 (3), 285–294. doi:10.1016/S1876-3804(12)60044-5

Stricker, S., Jones, S. J., Sathar, S., Bowen, L., and Norman, O. (2016). Exceptional reservoir quality in HPHT reservoir settings: Examples from the skagerrak formation of the heron cluster, north sea, UK. *Mar. Pet. Geol.* 77, 198–215. doi:10.1016/j.marpetgeo.2016.02.003

Sun, L., Zou, C., Zhu, R., Zhang, Y., Zhang, S., Zhang, B., et al. (2013). Formation, distribution and potential of deep hydrocarbon resources in China. *Pet. Explor Dev.* 40 (6), 687–695. doi:10.1016/S1876-3804(13)60093-2

Tian, J., Yang, H., Wu, C., Mo, T., Zhu, W., and Shi, L. (2020). Discovery of Well Bozi 9 and ultra-deep natural gas exploration potential in the Kelasu tectonic zone of the Tarim Basin. *Nat. Gas. Ind.* 40 (1), 11–19. doi:10.3787/j.issn.1000-0976.2020.01.002

Tian, X., Zhuo, Q., Zhang, J., Hu, H., and Guo, Z. (2017). Sealing capacity of the Tugulu Group and its significance for hydrocarbon accumulation in the lower play in

the southern Junggar Basin, northern China. *Oil Gas. Geol.* 38 (2), 334–344. doi:10.11743/ogg20170213

Tingay, M. R. P., Hillis, R. R., Swarbrick, R. E., Morley, C. K., and Damit, A. R. (2009). Origin of overpressure and pore-pressure prediction in the Baram province, Brunei. *AAPG Bull.* 93 (1), 51–74. doi:10.1306/08080808016

Wang, B., Qiu, N., Duan, Y., and Littke, R. (2022). Modelling of pore pressure evolution in a compressional tectonic setting: The Kuqa Depression, Tarim Basin, northwestern China. *Mar. Pet. Geol.* 146, 105936. doi:10.1016/J.MARPETGEO.2022.105936

Wang, W., Pang, X., Wu, L., Chen, D., Huo, Z., Pang, Y., et al. (2015). Pressure distribution features of deep and middle-shallow hydrocarbon reservoir in global oil and gas-bearing basins. *Acta Pet. Sin.* 36 (2), 194–202. doi:10.7623/syxb2015S2018

Wang, X., Bai, B. J., Lu, H., Liang, Z., Zhao, C., Hu, Y., et al. (2022). Characteristics and main controlling factors of deep and ultra-deep glutentite reservoirs with high temperature and very strong overpressure: A case study from the cretaceous Qingshuihe Formation in gaoquan area, Sikeshu sag, southern margin of Junggar Basin. *J. Northeast Pet. Univ.* 46 (3), 54–65. doi:10.3969/j.issn.2095-4107.2022.03.005

Wang, X., Wang, X., Liu, J., and Ma, Y. (2005). Analysis of the fold thrust zone in the southern Junggar Basin north Western China. *Earth Sci. Front.* 12 (4), 411–421.

Wang, Z., Luo, X., and Chen, H. (1997). Rebuilding of palaehydrodynamic field in sedimentary basin: Principle and means. *J Northwest U Nat. Sci. Ed.* 27 (2), 155–159.

Wang, Z., Sun, M., Geng, P., Song, Y., and Li, Y. (2003). The development features and formation mechanisms of abnormal high formation pressure in southern Junggar region. *Pet. Explor Dev.* 30 (1), 32–34.

Wei, D., Zhao, Y., AbulimitiChen, T., Yang, H., Wu, L., and Li, S. (2010). Difference of hydrocarbon accumulation in the foreland thrust-fold belt of the southern Junggar Basin. *Geol. J. China U* 16 (3), 339–350. doi:10.3969/j.issn.1006-7493.2010.03.007

Wu, X., Wang, L., and Song, Z. (2000). The relations between structural stress field and hydrocarbon migration and accumulation in southern margin of Junggar Basin. *Xinjiang Pet. Geol.* 21 (2), 97–100.

Xu, G., Kuang, J., Li, J., and Dang, L. (2000). Research on the Genesis of abnormal high pressure in the foreland basin to the north of Tianshan. *J. Chengdu U Techno* 27 (3), 255–262.

Yang, G., Li, W., Li, B., and Wang, X. (2012). Activity thrust faults and overpressure in the thrust and fold belt of southern Junggar Basin. *Chin. J. Geol.* 47 (3), 669–684.

Yang, X., Mao, Y., Zhong, D., Li, Y., Neng, Y., Sun, H., et al. (2016). Tectonic compression controls the vertical property variation of sandstone reservoir: An example of Cretaceous Bashijiqike Formaion in Kuqa foreland thrust belt, Tarim Basin. *Nat. Gas. Geosci.* 27 (4), 591–600. doi:10.1902/jop.2015.150390

Yu, Y., Yang, T., Guo, B., Zhan, L., Xu, X., and Yang, C. (2019). Major advances and outlook for oil and gas exploration, theory and technology of foreland thrust belts in China. *Acta Geol. Sin.* 93 (3), 545–564. doi:10.19762/j.cnki.dizhixuebao.2019063

Yuan, G., Cao, Y., Jia, Z., Wang, Y., and Yang, T. (2015). Research progress on anomalously high porosity zones in deeply buried clastic reservoirs in petroliferous basin. *Nat. Gas. Geosci.* 26 (1), 28–42. doi:10.11764/j.issn.1672-1926.2014.01.0028

Zhang, F., Lu, X., Scott, B., Murray, G., Zhuo, G., Zhuo, Q., et al. (2021). Horizontal tectonic stress as a cause of overpressure in the southern margin of the Junggar Basin, northwest China. *J. Pet. Sci. Eng.* 205, 108861. doi:10.1016/J.PETROL.2021.108861

Zhang, F., Lu, X., Zhuo, Q., Zhong, H., Zhang, P., Wei, C., et al. (2020). Genetic mechanism and evolution characteristics of overpressure in the lower play at the southern margin of the Junggar Basin, northwestern China. *Oil Gas. Geol.* 41(5), 1004–1016. doi:10.11743/ogg20200511

Zhang, F., Wang, Z., Song, Y., Zhao, M., Fan, C., and Zhao, X. (2012a). Study of impact of tectonic compaction on natural gas migration and accumulation in Kuqa foreland basin. *Geo Rev.* 58 (2), 268–276.

Zhang, F., Wang, Z., Song, Y., Zhao, M., Liu, S., Fang, S., et al. (2011). On design and implementation of neural-machine interface for artificial legs. *J China U Pet Ed. Nat. Sci.* 35, 1–7. doi:10.1109/TII.2011.2166770

Zhang, F., Wang, Z., Zhao, X., and Song, Y. (2012b). Genetic mechanism of overpressure and its relationship with hydrocarbon accumulation in Dina-2 gasfield, Kuqa depression. *Acta Pet. Sin.* 33 (5), 739–747.

Zhang, G., Ma, F., Liang, Y., Zhao, Z., Qin, Y., Liu, X., et al. (2015). Domain and theory-technology process of global deep oil and gas exploration. *Acta Pet. Sin.* 36 (9), 1156–1166. doi:10.7623/syxb20150901

Zou, C., Zhai, G., Zhang, G., Wang, H., Zhang, G., Li, J., et al. (2015). Formation, distribution, potential and prediction of global conventional and unconventional hydrocarbon resources. *Pet. Explor Dev.* 42 (13), 14–28. doi:10.1016/S1876-3804(15)60002-7